Power Spectrum Estimation for Frequency Domain Ambient Modal Analysis and Oscillation Monitoring

Chad Thomas, Mohammadreza Maddipour Farrokhifard and Vaithianathan "Mani" Venkatasubramanian
Washington State University, Pullman, WA, USA, Email: mani@wsu.edu

Abstract

This paper studies the effect of Power Spectrum Density (PSD) estimation techniques on the accuracy of Fast Frequency Domain Decomposition (FFDD). FFDD utilizes ambient synchrophasor measurements to estimate characteristics of dominant system modes by analyzing the PSD matrix from multiple synchrophasor measurements. In this paper, impact of three different methods for PSD estimation on the accuracy of FFDD modal estimates is investigated: Welch Periodogram (PWelch), MultiTaper Method (MTM) using Slepian Tapers, and MTM using Sine Tapers. Tests are done using synthetic and archived synchrophasor data. All three methods are shown to work well for oscillation detection of sustained oscillations using FFDD. However, for ambient modal analysis, it is shown that FFDD based on MTM with Slepian Tapers has the most reliable modal estimations. FFDD using both MTM with Sine Tapers and PWelch have bias issues in estimating well-damped system modes, requiring more research for them to be suitable for FFDD.

1. Introduction

Oscillation monitoring in the power grid has been a growing research area for many years. Poorly-damped oscillations, when left uncorrected, can cause damage to electromechanical machinery or can lead the system to wide-spread blackouts, such as the August 10, 1996 event of the North American Western Interconnection (WECC) grid [1,2]. Therefore, accurate methods to monitor and control these oscillations in the power grid are important for maintaining power system stability and operational reliability.

The characteristics of power systems low-frequency oscillations can be estimated through model-based linearization methods [3] or measurement-based methods [4,5]. However, accurate models of power systems are not always available, making measurement-based methods more attractive. Furthermore, widespread implementation of synchrophasor devices across many power grids allow measurement-based methods to analyze system characteristics in real-time.

There are numerous methods for measurement-based modal analysis of power systems which can be mainly categorized as ringdown and ambient types (e.g. [7-10,11-15]). Ringdown analysis techniques are post-disturbance methods that use the oscillatory response of the system after an event (such as line tripping or generator outage) to estimate the excited modes [6]. Some of the prominent ringdown analysis methods are Prony [5,7], Matrix Pencil [8], Hankel Total Least Squares (HTLS) [5], and Eigen-system Realization Algorithm (ERA) [9,10]. While these methods can be very accurate due to the relatively large magnitude of the oscillations, they require system responses following disturbances and therefore, are not suitable for providing continuous system mode estimations.

On the other hand, ambient analysis methods rely on the response of the system operating in quasi-steady-state conditions when the main excitation of the system is small random variations in loads being formulated as white noise [6]. In contrast with ringdown data, the ambient data is always available and therefore is much better suited for real-time measurement-based oscillation monitoring. Ambient modal analysis methods can be categorized into time- and frequency-domain algorithms. Time-domain methods proposed by researchers include robust RLS first introduced in [11], Modified Extended Yule-Walker (MEYW) in [12], and Stochastic Subspace Identification (SSI) in [13].

Frequency Domain Decomposition (FDD) is a popular frequency domain ambient modal analysis method that was extended to power system ambient oscillation monitoring in [14]. The main idea behind FDD method is to apply Singular Value Decomposition (SVD) to the power spectrum matrix estimated from ambient measurements. Furthermore, [15] proposed the Fast Frequency Domain Decomposition (FFDD) algorithm which does not require the SVD calculation, making the method faster for real-time application. One of the key steps in both FDD and FFDD is the estimation of the power spectrum from measurements. Due to the real-time application of these methods, analysis window length should be sufficiently short which generally increases the PSD estimation leakage. Therefore, power spectrum estimation methods that have minimal bias with good frequency resolution while not being computationally intensive are desirable to mitigate the leakage.

URI: https://hdl.handle.net/10125/79763
978-0-9981331-5-7

The FFDD algorithm proposed in [15] is based on the Slepian MultiTaper Method (Sl-MTM) for power spectrum estimation. However, other PSD estimation methods such as the Sine Taper based MultiTaper Method (Si-MTM) and PWelch have been proposed for different applications with varying advantages. The Sine Taper Method in [16] was shown to have bias improvements over the Slepian Taper method. Furthermore, PWelch is popular because of its simplicity of implementation and suppressed spectrum sidelobes [17,18]. Both Slepian and Sine Tapers are MultiTaper methods, utilizing the periodograms of weighted frequency windows (also called tapers) to estimate the Power Spectral Density (PSD) function of a dataset. However, the Slepian and Sine methods both differ in the weighting functions of the frequency tapers. PWelch utilizes Fast Fourier Transform (FFT) calculations from overlapping time windows to estimate the overall PSD of signals [17]. These methods will be discussed in more detail in Section 2.

In this paper, we comprehensively study the performance of FFDD method in estimating system modes when Slepian Taper, Sine Taper, and PWelch methods are utilized for the PSD estimation step in this algorithm. In order to have the best performance of the FFDD in tracking modes, the parameters of PSD estimation techniques need to be properly tuned. To do so, a set of archived measurements from phasor measurement units (PMUs) during a recent forced oscillation event in the WECC grid is utilized. The performance of the FFDD with optimized PSD estimators is examined and compared with each other as well as with the time-domain SSI method using synthetic and real archived PMU data. Covariance-based SSI [23,24] has an advantage that it can detect natural modes together with interacting forced oscillations simultaneously. However, SSI is computationally far more intensive [24] compared to FFDD and also has the problem that some of the modal estimates may be spurious. It is shown that the FFDD with all three PSD estimators has small bias for estimating the damping ratio of sustained or forced oscillations. However, the FFDD with Slepian Taper method has the least bias for estimating the damping ratio of well-damped modes in comparison with the FFDD with the two other PSD estimators.

The rest of the paper is organized as follows: Section 2 discusses FDD along with FFDD. Then, it overviews the three PSD estimation methods: Slepian Tapers, Sine Tapers, and PWelch. Parameter tuning for each method is conducted in Section 3. The performance of the FFDD with all three PSD estimators along with SSI method is compared using synthetic and real PMU data in Section 4. Section 5 concludes the paper.

2. FDD, FFDD and PSD Estimation Methods Theory

2.1. FDD and FFDD Algorithms

The power grid model, being a high-order nonlinear system, can be linearized around an operating equilibrium point. The resulting state-space equations can be represented as follows [3]:

$$\begin{aligned} \Delta\dot{x} &= A\Delta x + B\Delta u \\ \Delta y &= C\Delta x \end{aligned} \quad (1)$$

where Δx is the linearized dynamic state vector, Δy is the linearized output vector, and Δu is the linearized input vector. Given a stationary random process x(t), the autocorrelation function is defined as $\gamma_{xx}(\tau) = E[x^*(t)x(t+\tau)]$ with the superscript * denoting the complex conjugate transpose. Taking the Fourier Transform of this autocorrelation function results in $S(j\omega)$, the PSD of $x(t)$ according to the Wiener-Khintchine theorem [3, Page 285]. For a multi-input multi-output (MIMO) system, the output PSD matrix $S_{yy}(j\omega)$ can be defined as

$$S_{yy}(j\omega) = H(j\omega) \cdot S_{uu}(j\omega) \cdot H^*(j\omega) \quad (2)$$

where $H(j\omega)$ is the $n_y \times n_u$ transfer function and $S_{uu}(j\omega)$ is the $n_u \times n_u$ input PSD matrix. With the input being white noise, $S_{uu}(j\omega)$ will be a constant diagonal matrix. Furthermore, $S_{yy}(j\omega)$ is estimated directly from synchrophasors and PMU signals.

Taking the SVD of the output PSD matrix near the frequency ω_i of a mode $\lambda_i = -\alpha_i + j\omega_i$ results in

$$\hat{S}_{yy}(j\omega_i) = W_i(j\omega_i) \cdot S_i(j\omega_i) \cdot W_i^*(j\omega_i) \quad (3)$$

with $W_i(j\omega_i)$ being a matrix of singular vectors and $S_i(j\omega_i)$ being the corresponding singular values. In the case that there is one dominant mode near the frequency ω_i, the first singular value in $S_i(j\omega_i)$ will be much larger in magnitude compared to the other singular values. In compiling all of these main singular values in terms of their frequency ω_i, the Complex Mode Identification Function (CMIF) can be formulated [14]. By taking the Inverse FFT of CMIF near the peak frequency, ringdown analysis methods such as Prony Method and HTLS can be utilized to estimate the frequency and damping of the mode near the peak frequency ω_i.

A modified FDD algorithm titled Fast Frequency Domain Decomposition (FFDD) was proposed in [15] to circumvent the computationally burdensome SVD

calculations. The main idea of FFDD is to approximate the largest singular value of $S_i(j\omega_i)$ by the sum of the individual autocorrelation estimates. Whereas FDD needs multiple SVD calculations utilizing both auto- and crosscorrelation estimates to estimate $\hat{S}_{yy}(j\omega_i)$ that constitute the CMIFs, FFDD approximates CMIFs directly from the sum of autocorrelation estimates [15]. In this regard, FFDD is much less computationally burdensome than FDD and is better suited for real-time oscillation monitoring. With the CMIFs, FFDD follows the same procedure as FDD, taking the inverse FFT and conducting ringdown analysis to estimate the system modes [14,15].

A critical part of FFDD is estimating the PSD matrix through the FFTs of the input dataset. In taking the FFT of raw synchrophasor data, some information could be lost due to leakage from the finite analysis window. Because of this, the data is crucially multiplied by a filtering window before FFT is conducted for reducing the leakage. However, this can affect the performance of the FFDD estimation depending on the PSD estimation method used. This paper tests three different methods that filter the FFT for estimation of the power spectrum.

2.2. PSD Estimation Methods

As mentioned in the previous section, the PSD estimation is one of the key steps in the process of the modal estimation by FFDD method. The three methods compared in this paper are PWelch, Sl-MTM, and Si-MTM.

PWelch calculates the PSD of the data through splitting the dataset into K overlapping windows and averaging the individual window FFT estimates [17]. Through overlapping windows, leakage of the PSD estimation is decreased. Furthermore, windowing functions such as Hanning, Hamming, or Blackman can be utilized to filter the split windows and smooth the overall power density estimate, depending on the windowing function used [19].

However, if the overlapping windows are short in length, this can create a significant bias in the modal estimate. The advantage of PWelch is that it is a robust algorithm and easily implementable. Furthermore, the windowing function can be altered depending on the desired properties of side lobes. Therefore, PWelch is a simple method to reduce leakage and creates a smooth PSD estimate, although can suffer from bias issues.

The MultiTaper Method (MTM) by Thomson is presented in [20]. Through utilizing multiple orthogonal frequency windows (called tapers or spectral estimators) to calculate weighted FFTs, MTM gets multiple independent spectrum estimates with the same input dataset. The set of tapers almost exclusively used in MTM are Slepian Tapers, also called Discrete Prolate Spheroidal Sequences (DPSS) [20]. Each taper n, denoted as $v_n^{(k)}(N,W)$ with $k = 0,1,\dots,N-1$, is the solution to a Toeplitz eigenvalue matrix,

$$\sum_{m=0}^{N-1} \frac{\sin 2\pi W(n-m)}{\pi(n-m)} \cdot v_n^{(k)}(N,W) = \lambda_k(N,W) \cdot v_n^{(k)}(N,W) \quad (4)$$

where W is the bandwidth of the function, N is sequence length, and $\lambda_k(N,W)$ are the eigenvalues of DPSS. Because the tapers drop in magnitude further from the target frequency, DPSS tapers maximize their spectral concentration within the bandwidth $[-W,W]$. More information on DPSS tapers can be found in [25].

With the solved DPSS values, the taper spectral estimates can be calculated through

$$\hat{S}_k(j\omega) = \frac{1}{N}\left|\sum_{n=0}^{N-1} x(n) \cdot v_n^{(k)}(N,W) \cdot e^{-j2\pi fn}\right|^2 \quad (5)$$

with $x(n)$ being the input dataset from 0 to $N-1$. All of the spectral estimates can then be averaged together to estimate the PSD of the system. While Slepian or DPSS Tapers optimize the spectral density of the frequency windows, Sine Tapers are supposed to minimize the bias of the windowing [21]. With the local bias being proportional to the leading term of the PSD bias, the bias is reduced through tapers that minimize $\int_{-1/2}^{1/2} |V(f)|^2 f^2 df$. Sine Tapers are defined as

$$v_n^{(k)} = \sqrt{\frac{2}{N+1}} \sin\left(\frac{\pi kn}{N+1}\right), k = 1,2,\dots,N \quad (6)$$

MTM is effective at analyzing multiple orthogonal datasets from a single input time sequence, making estimations quite accurate. Furthermore, Slepian Tapers optimize the spectral density of the frequency windows while Sine Tapers are expected to minimize the bias in the estimations. However, MTM performance is sensitive to variations in parameters such as time half bandwidth product (NW) and FFT length (N), making it less robust in varied applications.

3. Tuning Using a Field Event

On September 5, 2015, the western electricity coordination council (WECC) or the western grid had an oscillation event in which a forced oscillation near 0.4 Hz suddenly appeared, lasting approximately 9 minutes. This forced oscillation resonated with the well-

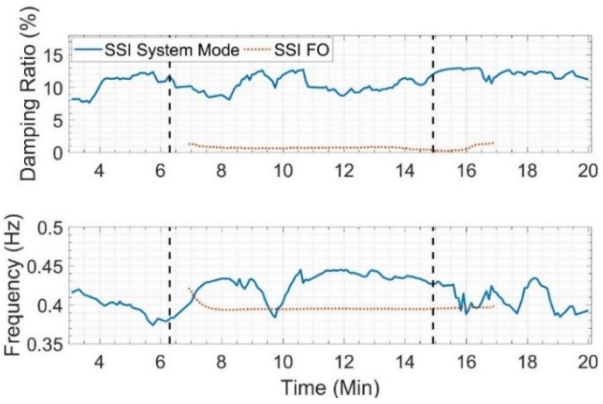

Figure 1. SSI damping ratio and frequency estimates for both the system mode and forced oscillation utilizing a WECC forced oscillation dataset.

known 0.4 Hz North-South interarea system mode resulting in widespread oscillations. In this section, archived synchrophasor data of this event is utilized to select reasonable settings for Si-MTM and PWelch. A commercial oscillation monitoring tool titled Damping Monitor Offline (DMO) [22] from Washington State University (WSU) already utilizes Slepian Tapers in the FFDD algorithm. As such, the performance of the Slepian taper based MTM used in FFDD of DMO will be compared to Si-MTM and PWelch based FFDD implementations. Different PSD estimates are then processed by DMO to estimate CMIF and the dominant system mode frequencies and damping ratios as in the FFDD algorithm [22].

An ideal FFDD modal analysis engine should reliably track both well-damped system modes during normal ambient conditions and poorly-damped forced oscillations during stressed operating conditions. For this forced oscillation event, the actual damping ratio for the WECC 0.4 Hz mode is not exactly known being from a real system. In this context, we use the estimates of the well-known time-domain method, covariance based SSI [23, 24] which is also implemented in DMO [22].

Figure 1 shows the frequency and SSI damping ratio estimates for the WECC forced oscillation event. The two vertical dashed lines indicate the beginning and end of the event, respectively. A crucial advantage of SSI is that the method can simultaneously track the presence of both the system mode and an interacting forced oscillation during such events [23]. The "SSI FO" plot shows the estimates of the forced oscillation while "SSI System Mode" shows the estimates of the 0.4 Hz system mode. As seen in the results, SSI is consistently estimating the system mode at around 10% damping ratio and the damping ratio of the forced oscillation estimates is nearly zero.

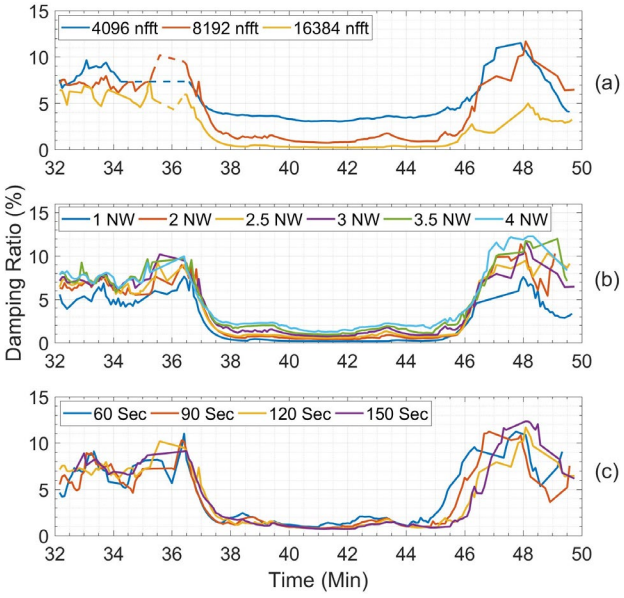

Figure 2. Tuning plots for Sine Taper method utilizing WECC forced oscillation dataset. Plot (a) varies number of points in FFT calculation, plot (b) changes NW, and plot (c) compares different analysis window lengths.

Accordingly, we expect the damping ratio estimates of FFDD to be around 10% before and after the forced oscillation event. Unlike SSI, FFDD being a frequency domain method combines the effects of the forced oscillation and the 0.4 Hz system mode during the event when the forced oscillation is present. Since the energy of the system response from the forced oscillation is expected to dominate over the ambient modal response of the well-damped system mode, we expect FFDD to produce near zero damping ratio estimates when the forced oscillation is present in the system. The three PSD estimation methods will be tuned in this section to match these damping ratio estimations before (near 10%), during (near 0%) and after (near 10%) the forced oscillation event.

Figure 2 shows the tuning plots for MTM using Sine Tapers. Plot (a) compares the number of points used for the FFT calculation in the method (nfft). Plot (b) compares differing taper windows through the NW variable for the best nfft value. Finally, the analysis window is adjusted in plot (c) using the best previous settings. Dashed lines in the plots signify gaps in mode estimations where the method could not estimate the 0.4 Hz mode because of spectral issues.

It can be seen in plot (a) of Figure 2 that an nfft value of 4096 has a large bias during the event, estimating the damping ratio to be around 3%. Furthermore, the 16384 nfft damping estimations do not properly recover after the event. Therefore, an nfft

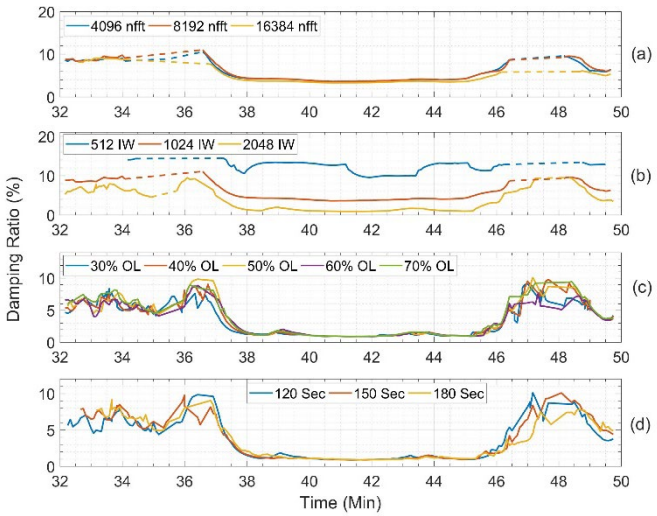

Figure 3. Tuning plots for PWelch method utilizing WECC forced oscillation dataset. Plot (a) varies number of points in FFT calculation, plot (b) changes number of points in inner window, plot (c) alternates window overlap percentage, and plot (d) compares different analysis window lengths.

length of 8192 is chosen as the recommended nfft setting. In plot (b) of Figure 2, NW had minimal variability in the damping estimations. Because of this, an NW value of 3 was chosen due to the more accurate pre-event damping ratio estimates. In plot (c) of Figure 2, it can be seen that an analysis window length of 90 seconds had good estimate trends while recovering post-event to higher damping ratios quickly. The final recommended settings for FFDD with Sine Tapers are namely, 8192 for nfft, 3 for NW, and 90 seconds for the analysis window length.

Figure 3 shows the tuning figures for the PWelch method. The same methodology as Sine Tapers was conducted, only with nfft, inner window length (IW), overlap percentage (OL), and analysis window length. From plot (a), an nfft length of 8192 had the highest pre- and post-event damping estimates while maintaining equivalent event bias, making it the suitable setting. For plot (b), an inner window length of 2048 was chosen due to the minimal bias during the event and the increased quantity of estimates. Overlap percentage had little effect on damping estimations. Therefore, an overlap percentage of 50% was chosen due to the slightly higher pre-event damping estimates. Plot (d) shows the 150-second analysis window length having slightly better overall damping estimates. Therefore, the final settings chosen for PWelch are 8192 for nfft, 2048 for IW, 50% for OL, and 150 seconds for analysis window length.

Although Slepian Taper method settings are defined internally for FFDD [22], Figure 4 shows the Slepian Taper method damping ratio estimations with varying analysis window lengths. While a 90-second

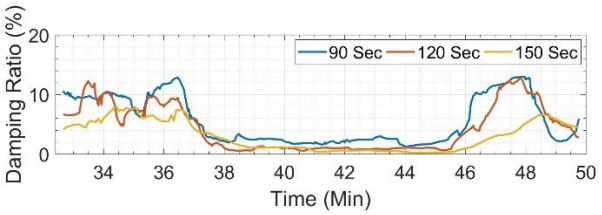

Figure 4. Tuning plot for Slepian Taper method utilizing WECC forced oscillation dataset.

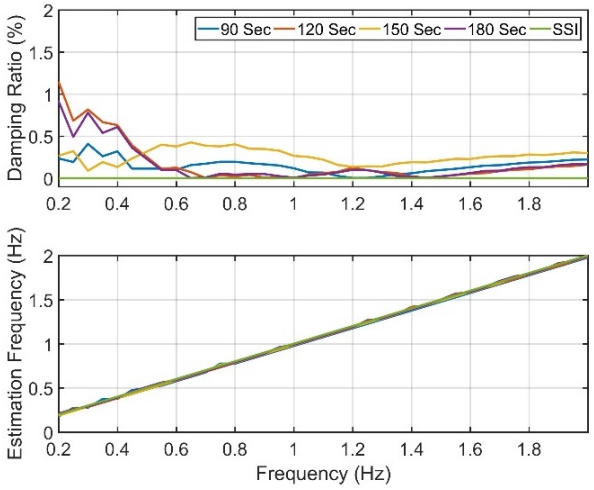

Figure 5. Synthetic sinusoidal forced oscillation frequency and damping ratio estimates for FFDD with Slepian Taper method.

analysis window length had 10% damping ratio estimations for the 0.4 Hz mode before the event, there was significant bias in the estimation of damping ratio when the forced oscillation appears in the system. Due to this, an analysis window length of 120 seconds was chosen for Slepian Taper method for the combination of good pre and post-event damping ratio estimations.

It appears that there may have been other unknown forced oscillations with frequencies near 0.4 Hz present in the system for the time period starting around 48 seconds in Figures 2, 3 and 4 which may be causing low damping ratio estimates among all the FFDD estimations. This requires further investigation.

4. Synthetic and Field Case Studies

In this section, results of FFDD using all three PSD estimation methods are analyzed first for a set of simulated sustained forced oscillation signals. Then, the methods are compared by analyzing archived WECC event data including the forced oscillation event of Section 3 and a WECC brake test. The tuned settings from Section 3 are used for each method in the case studies. Forced oscillations are sustained oscillations caused by external mechanisms [23] and can interact with system modes. However, presence or detection of

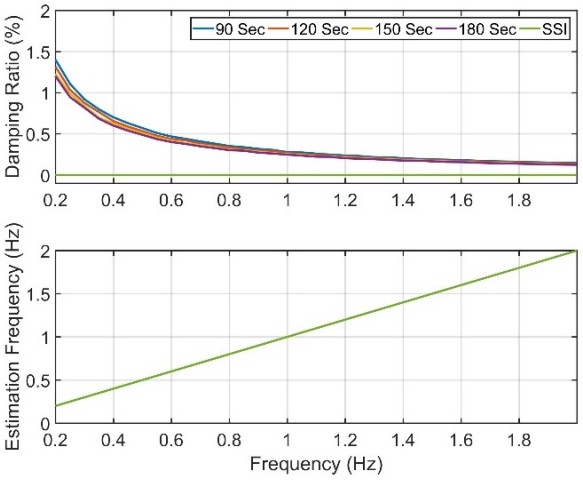

Figure 6. Synthetic sinusoidal forced oscillation frequency and damping ratio estimates for FFDD with Sine Taper method.

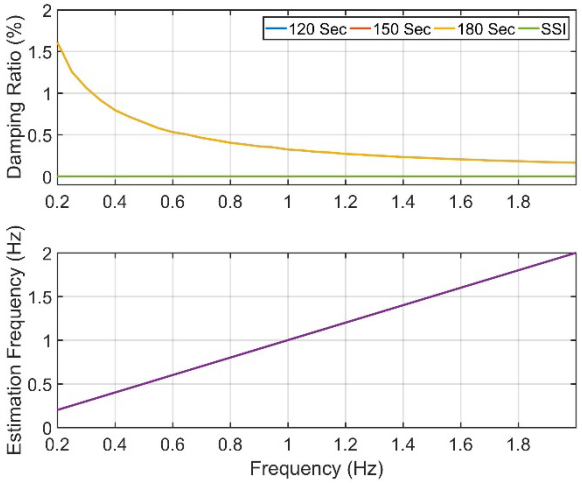

Figure 7. Synthetic sinusoidal forced oscillation frequency and damping ratio estimates for FFDD with PWelch method.

forced oscillations by itself does not imply presence of poorly damped natural modes in the system.

4.1. Synthetic Sustained Oscillation Case Study

In this case study, a range of simulated sustained forced oscillation signals are utilized to compare the PSD estimation methods. The synthetic oscillation frequencies are varied between 0.2 Hz and 2 Hz, with a step size of 0.05 Hz. Furthermore, the sampling frequency of the input dataset is set at 30 Hz. The analysis window is also tested at 90, 120, 150, and 180 seconds to evaluate the performance difference with a larger sample size. The main objective of testing with simulated sustained forced oscillations is to evaluate the bias of the damping ratio estimates, as a sustained forced oscillation without noise should have a damping ratio of 0%. SSI algorithm frequency and damping ratio estimates are also shown as a benchmark for the PSD estimation methods. The SSI settings utilized for all case studies in this paper are 240-second analysis window, system order of 20, and 6-second inner window length.

Figure 5 shows the frequency and damping ratio estimates for FFDD with the Slepian Taper method. It can be seen that the bias of the damping ratio estimations generally decreases with a larger oscillation frequency. Furthermore, it can be seen that estimation bias also generally decreases with a larger analysis window. Since there is more input data to make an estimation with, the mode estimations are more accurate. While the SSI damping ratio estimates were a consistent 0%, the Slepian Taper estimates had a maximum bias of 1% for the 0.2 Hz sinusoidal signal. Furthermore, Slepian Taper frequency estimates matched well with SSI frequency estimates.

Figure 6 shows the frequency and damping ratio estimates for FFDD with the Sine Taper method. The settings for each analysis window length were the same optimized settings from Section 4 of this paper. As previously seen, the bias of the damping ratio estimations decreases with a larger oscillation frequency. Furthermore, it can be seen that estimation bias also decreases with a larger analysis window, similar to Slepian Taper method. The Sine Taper estimates had a maximum bias of 1.5% for the 0.2 Hz sinusoidal signal compared to the SSI damping ratio results. The frequency estimates varied from the actual frequency and SSI frequency by approximately 0.001 Hz, showing that for a noiseless system the frequency estimates are very accurate. Overall, these forced oscillation results compare well with the Slepian Taper method and SSI, showing the viability of the Sine Taper method for this case study.

Figure 7 shows the frequency and damping ratio estimates for FFDD with the PWelch algorithm. The settings for each analysis window length were the same optimized settings from Section 3 of this paper. As with the Slepian and Sine Tapers, it can be seen that the estimation bias decreases as the oscillation frequency increases. Furthermore, damping estimation is comparable to both MultiTaper methods and SSI with a maximum bias of 1.55% for the 0.2 Hz sinusoidal signal. However, unlike the other methods, damping ratio estimations do not change with different analysis window lengths. By changing the analysis window length there are simply more windows of the same estimate instead of additional data being used to estimate the mode at any single time. Finally, PWelch frequency estimates exactly match the actual and SSI frequency estimates. Like the other two methods, these

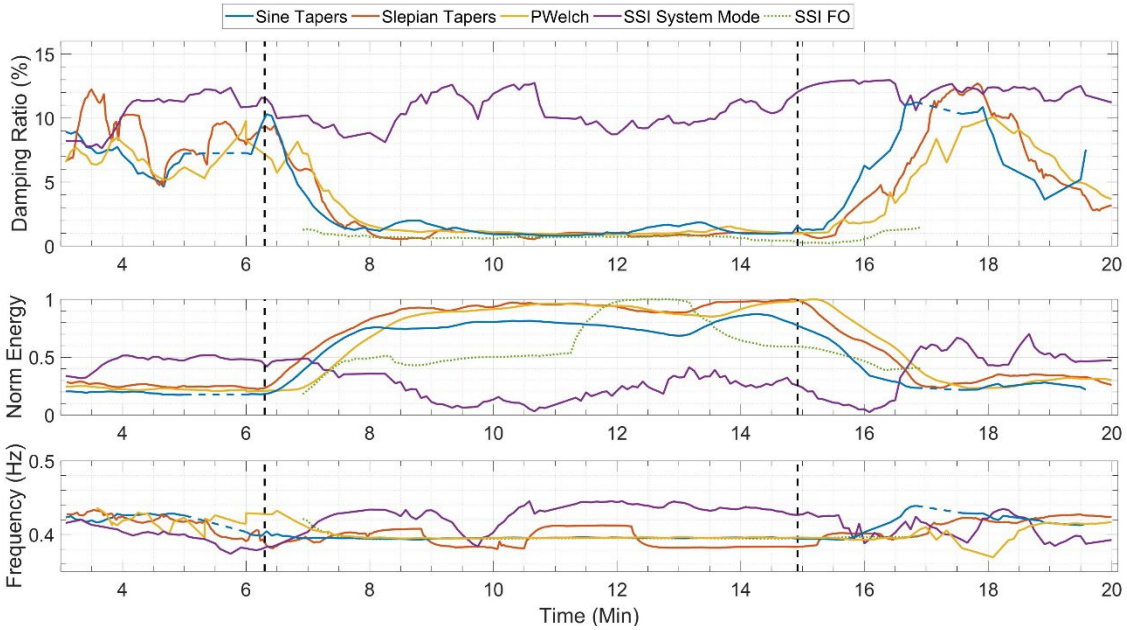

Figure 8. 0.4 Hz WECC estimates for the Sept. 15, 2015 forced oscillation event.

PWelch estimations show viability for this synthetic modal analysis case.

4.2. WECC Forced Oscillation Case Study

Figure 8 shows the 0.4 Hz estimations for all three FFDD methods within a 17-minute window for the WECC forced oscillation event. All methods are using the final tuned settings from the results of Section 3. Figure 8 also includes two estimates for the SSI algorithm for reference. The "SSI FO" curve follows the forced oscillation while "SSI System Mode" maintains estimates for the interarea mode. The vertical dashed lines signify the start and end of the forced oscillation event.

It is seen that all three methods have similar response times of approximately 1.5 minutes after the event started. Furthermore, the damping ratio estimations during the event for all three FFDD methods are at about 0.5%, matching very well with the SSI FO results. Before the event occurs, all three FFDD damping ratio estimations are in the 6% to 10% range. Although that is lower than the estimated 11% for SSI, this may be from the presence of other unknown forced oscillations in the WECC data as noted earlier. The post-event damping ratio estimates for both MTM methods are higher at 11 to 12%, very close to the SSI estimate. PWelch recovered to a damping ratio estimate of 9% to 10%.

Furthermore, as expected, the estimation energy for all three methods increases significantly during the event from capturing the effect of the system response to the 0.4 Hz forced oscillation. The SSI system mode

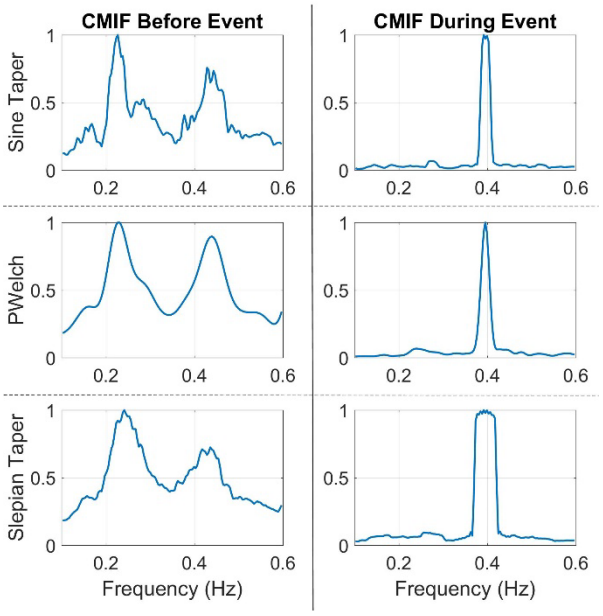

Figure 9. CMIF plots for FFDD methods before and during forced oscillation event.

energy does not increase for the event since it can distinguish between the forced oscillation and the system well-damped mode as two separate estimates.

Figure 9 shows the CMIF shapes for all three methods before and during the forced oscillation event. Before the event under normal ambient conditions, all three FFDD methods CMIF shapes are showing multiple system modes, including one at 0.23 Hz. However, as the forced oscillation with the frequency of 0.4 Hz appears in the system, the CMIF shapes clearly

Table 1. Average damping ratio and frequency estimates for ringdown analysis of the WECC brake test.

	Frequency (Hz)	Damping Ratio (%)
Prony	0.3938	11.485
Matrix Pencil	0.3889	11.6953
HTLS	0.3973	11.2134
ERA	0.3891	11.7022

highlight 0.4 Hz with all other modes decreasing in magnitude.

Overall, all three methods have accurate damping ratio estimations and low bias during the event, showing viability for this case study. This is to be expected as the settings for all three methods settings were tuned for this dataset in Section 3. However, FFDD with Slepian Taper method had more mode estimates compared to the other two methods.

4.3. WECC Brake Test Case Study

In this case study, a Chief Joseph brake test dataset on the WECC power grid is analyzed. The data is analyzed by the three different FFDD methods as well as SSI. Furthermore, the ringdown portions of the events are analyzed separately. Having the modal estimates of all these methods can lead us to a better and more accurate comparison.

The brake test was enacted by temporarily connecting a 1,400 MW resistive load to the Chief Joseph power generator terminal, initiating an impulse type disturbance in the system. This is intended to damp power swings following faults near the generator plant. However, during the brake tests, the resistive brake load is inserted to effect a ringdown response for assessing system small-signal properties and to conduct power system model validation studies. This also allows ringdown modal analysis techniques such as Prony or HTLS to be applied for getting an accurate estimate of the dominant system modes that are excited by the brake test. As FFDD is an ambient analysis technique, the three methods with FFDD will be conducted both during and after the event for ensuring ambient system conditions. These estimations will be compared with multiple ringdown analysis methods of the brake test itself along with SSI estimations.

Table 1 shows the average estimations of four ringdown methods during the brake test event for the 0.4 Hz interarea WECC mode. The four methods are Prony method, Matrix Pencil, HTLS, and ERA. The frequency estimations for all ringdown methods are very consistent centering at 0.397 Hz. Furthermore, the damping ratio estimations are around 11.4%. While this is higher than the 10% damping ratio as seen in the previous test, it is to be expected that the damping ratio will slightly fluctuate for a well-damped mode. As such, these

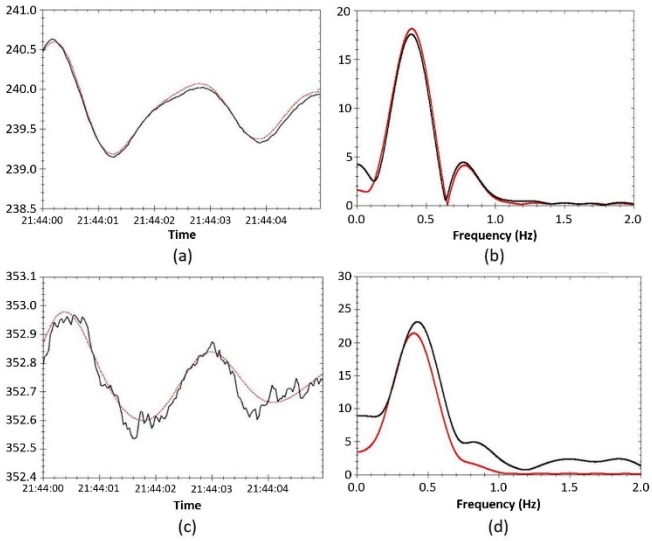

Figure 10. HTLS signal reconstruction (a and c) and FFT (b and d) where reconstruction is in red and actual signal in black for the brake test.

estimates are consistent with damping ratio estimates of the 0.4 Hz WECC interarea mode.

Plots (a) and (c) in Figure 10 show an actual signal in black compared to the reconstruction of the HTLS ringdown method in red. Plots (b) and (d) in Figure 10 show the FFT of both the actual signal in black and the HTLS reconstruction in red for the same signal. The HTLS model was determined through 118 input signals. Plots (a) and (b) are for the signal with the best fit in terms of the overall error while plots (c) and (d) are for the signal with the worst fit. Because the reconstructions closely fit the actual signals, it can be concluded that the ringdown estimations for this brake test are reasonable.

Figure 11 shows the ambient damping ratio estimations between FFDD with Slepian Tapers, Sine Tapers, and PWelch along with SSI estimations up to 16 minutes after the brake test. The same optimized settings for the WECC forced oscillation archived dataset are used for all methods. The vertical dashed line signifies the brake test. Variations in the damping ratio estimations are to be expected as they are based on stochastic ambient data modeled with random white noise inputs. However, it can be seen that both FFDD with Sine Tapers and PWelch have more variance in the damping ratio estimations compared with Slepian Tapers. Furthermore, both Sine Taper method and PWelch method have lower damping ratio estimations (larger bias) when compared to estimates of Slepian Taper method and SSI results.

As expected, the energy for each method increases during the brake test due to tracking the disturbance from the brake test. Furthermore, frequency estimates are consistently near 0.4 Hz for every method. It can

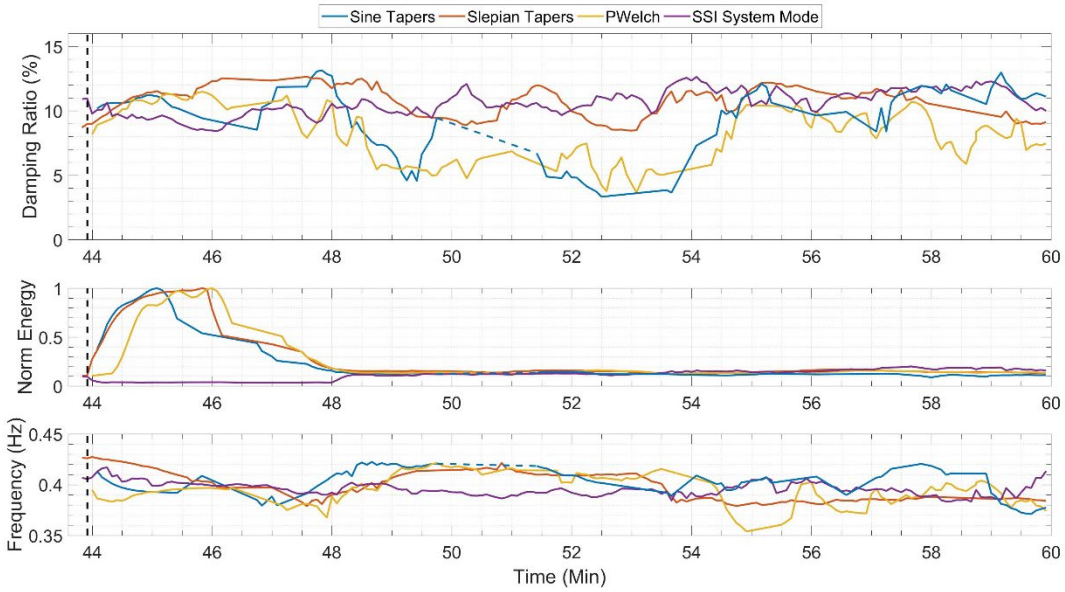

Figure 11. 0.4 Hz WECC estimates for the Chief Joseph brake test event.

Table 2. Average damping ratio and frequency estimates for ambient analysis of the WECC brake test.

	Damping Ratio (%)		Frequency (Hz)		Mode
Method	Avg	Std Dev	Avg	Std Dev	Observability
Sine Taper	9.3802	2.6539	0.4022	0.0139	50.26%
Slepian Taper	10.7864	1.1637	0.3988	0.0144	80.83%
PWelch	8.1395	2.0716	0.3943	0.0146	76.68%
SSI	10.5909	0.9638	0.3957	0.0065	96.89%

also be seen that immediately after the brake test the FFDD modal damping ratio estimates are very consistent. This is to be expected as the 0.4 Hz forced oscillation has high energy.

Table 2 shows damping ratio and frequency statistics for all three FFDD methods along with SSI for the brake test. The table also includes mode observability which signifies the percentage of windows with 0.4 Hz mode estimates during the analyzed time for each method. The frequency estimates for all methods are very similar, matching well with ringdown results from Table 1. For the damping ratio, the PWelch has the lowest average which shows significant bias in damping ratio estimates for the well-damped mode. Sine Taper method also has large bias in the damping ratio estimates while having the largest standard deviation. This signifies that the damping ratio estimates of the Sine Taper method have the largest variability during the analysis timeframe. The Slepian Taper method is closest to the SSI and ringdown results

It can further be seen that the Sine Taper method has several periods centered around 51 minutes without estimates. This is validated in Table 2 which shows that the Sine Taper method has significantly less mode observability than the other methods, indicating that this method is less reliable for this dataset.

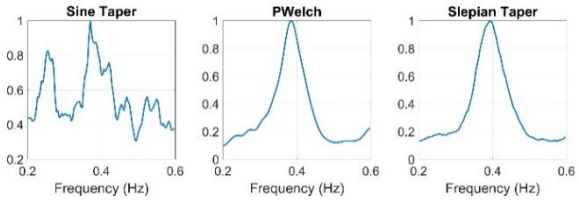

Figure 12. CMIF plots for FFDD methods under ambient conditions for the WECC brake test.

Figure 12 shows the ambient CMIF plots for all three FFDD methods. Similar to the WECC forced oscillation event, both PWelch and Slepian Taper method had the smoothest CMIF plots for 0.4 Hz. The Sine Taper CMIF plot has much greater noise and side lobes, explaining the low mode observability.

FFDD with Slepian Taper method has the closest damping ratio estimations to SSI and ringdown results for the WECC brake test. Furthermore, the mode observability is high due to the CMIF plots with defined 0.4 Hz peaks. FFDD with the PWelch method, while having similarly smooth CMIF plots, significantly underestimates the mode. FFDD with Sine Taper has marginal damping ratio estimation bias but has the lowest mode observability of the three methods.

5. Conclusion

In this paper, the suitability of different methods for PSD estimation such as PWelch, Sl-MTM, and Si-MTM for modal analysis using FFDD was investigated. It was determined that FFDD with Slepian Taper method performed well under synthetic sustained forced oscillations, having minimal bias in damping ratio

estimations. Furthermore, it showed consistency and accuracy in modal estimation for multiple real ambient datasets. Both Sine Taper method and PWelch, while they have certain advantages, require more research before they can be used for FFDD in oscillation monitoring.

As shown in the test studies in the paper, SSI methods have advantages compared to FFDD and there is a need for research on speeding up the time-domain methods such as SSI to enable them for efficient online implementations. Also, the studies show that the frequency domain methods such as FFDD are sensitive to the choice of spectral estimation methods and their parameters. Future research is indicated on developing automatic and optimal methods for tuning of the modal estimation algorithm parameters that work well in online implementations.

6. References

[1] D. N. Kosterev, C. W. Taylor, and W. A. Mittelstadt, "Model validation for the August 10, 1996 WSCC system outage," *IEEE Trans. Power Syst*., vol. 3, no. 4, pp. 967-979, Aug. 1999.

[2] V. Venkatasubramanian and Y. Li, "Analysis of 1996 Western American electric blackouts," in *Proc. Bulk Power System Dynamics and Control-VI*, Italy, 2004.

[3] P. Kundur, Power System Stability and Control. McGraw-Hill, Inc., New York, 1994.

[4] J. W. Pierre, D. J. Trudnowski, and M. K. Donnely, "Initial results in electromechanical mode identification from ambient data," *IEEE Transactions on Power Systems*, vol. 12, no 3, pp. 1245-1250, Aug. 1997.

[5] G. Liu, J. Quintero, and V. Venkatasubramanian, "Oscillation monitoring system based on wide area synchrophasors in power systems," in Proc. IREP, Aug. 19-24, 2007, *Bulk Power System Dyn. and Control-VII*.

[6] Z. Tashman, H. Khalilinia and V. Venkatasubramanian, "Multi-Dimensional Fourier Ringdown Analysis for Power Systems Using Synchrophasors," in *IEEE Trans. Power Systems*, vol. 29, no. 2, pp. 731-741, March 2014.

[7] J. F. Hauer,C. J. Demeure and L. L. Scharf, "Initial results in Prony analysis of power system response signals," in *IEEE Trans. Power Systems*, pp. 80-89, Feb. 1990.

[8] M. L. Crow and A. Singh, "The matrix pencil for power system modal extraction," in *IEEE Transactions on Power Systems*, vol. 20, no. 1, pp. 501-502, Feb. 2005.

[9] J.N. Juang and R. S. Pappa, "An eigensystem realization algorithm for modal parameter identification and model reduction," *J. Guidance, Control, Dynam. 8*, 1985.

[10] J. J. Sanchez-Gasca, "Computation of turbine-generator subsynchronous torsional modes from measured data using the eigensystem realization algorithm," 2001 *IEEE Power Engineering Society Winter Meeting. Conference Proceedings*, 2001, pp. 1272-1276 vol.3.

[11] N. Zhou, J. W. Pierre, D. J. Trudnowski and R. T. Guttromson, "Robust RLS Methods for Online Estimation of Power System Electromechanical Modes," in *IEEE Transactions on Power Systems*, vol. 22, no. 3, pp. 1240-1249, Aug. 2007.

[12] D. J. Trudnowski, J. W. Pierre, N. Zhou, J. F. Hauer and M. Parashar, "Performance of Three Mode-Meter Block-Processing Algorithms for Automated Dynamic Stability Assessment," in *IEEE Transactions on Power Systems*, vol. 23, no. 2, pp. 680-690, May 2008.

[13] H. Ghasemi, C. Canizares and A. Moshref, "Oscillatory stability limit prediction using stochastic subspace identification," in *IEEE Transactions on Power Systems*, vol. 21, no. 2, pp. 736-745, May 2006.

[14] Guoping Liu and V. Venkatasubramanian, "Oscillation monitoring from ambient PMU measurements by Frequency Domain Decomposition," 2008 *Proc. IEEE ISCAS*, Seattle, WA, 2008, pp. 2821-2824.

[15] H. Khalilinia, L. Zhang and V. Venkatasubramanian, "Fast Frequency-Domain Decomposition for Ambient Oscillation Monitoring," in *IEEE Transactions on Power Delivery*, vol. 30, no. 3, pp. 1631-1633, June 2015.

[16] M. A. Khan and J. W. Pierre, "Detection of Periodic Forced Oscillations in Power Systems Using Multitaper Approach," in *IEEE Transactions on Power Systems*, vol. 34, no. 2, pp. 1086-1094, March 2019.

[17] P. Welch, "The use of fast Fourier transform for the estimation of power spectra: A method based on time averaging over short, modified periodograms," in *IEEE Transactions on Audio and Electroacoustics*, vol. 15, no. 2, pp. 70-73, June 1967.

[18] A. T. Walden, "A unified view of Multitaper multivariate spectral estimation," *Biometrika*, vol. 87, no. 4, pp. 767-788, 2000.

[19] A. Nuttall, "Some windows with very good sidelobe behavior," in *IEEE Transactions on Acoustics, Speech, and Signal Processing*, vol. 29, no. 1, pp. 84-91, February 1981.

[20] D. J. Thomson, "Spectrum estimation and harmonic analysis," Proceedings of the IEEE, vol.70, no.9, pp.1055-1096, Sept. 1982.

[21] K. S. Riedel and A. Sidorenko, "Minimum bias multiple taper spectral estimation," in *IEEE Transactions on Signal Processing*, vol. 43, no. 1, pp. 188-195, Jan. 2018.

[22] *Damping Monitoring Offline*, Energy Systems Innovation Center, Wash. St. Univ., Pullman, WA, 2021.

[23] S.A.N. Sarmadi and V. Venkatasubramanian, "Electro-mechanical Mode Estimation Using Recursive Adaptive Stochastic Subspace Identification," *IEEE Trans. on Power Systems*, vol. 29, no. 1, pp. 349-358, Jan. 2014.

[24] T. Wu, V. M. Venkatasubramanian and A. Pothen, "Fast Parallel Stochastic Subspace Algorithms for Large-Scale Ambient Oscillation Monitoring," *IEEE Transactions on Smart Grid*, vol. 8, no. 3, pp. 1494-1503, May 2017.

[25] D. Slepian, "Prolate, spheroidal wavefunctions, fourier analysis and uncertainty v: the discrete case," *Bell System Technical Journal*, 57, 1371-1430, 1978.

Acknowledgements: The authors thank Power System Engineering Research Center and RTE, Paris, France for supporting this research work.